Stress deflections around salt diapirs in the Gulf of Mexico

ROSALIND KING[1]*, GUILLAUME BACKÉ[2], MARK TINGAY[2], RICHARD HILLIS[3] & SCOTT MILDREN[4]

[1]*Centre for Tectonics, Resources and Exploration (TRaX), School of Earth and Environmental Sciences, University of Adelaide, SA 5005, Australia*

[2]*Centre for Tectonics, Resources and Exploration (TRaX), Australian School of Petroleum, University of Adelaide, SA 5005, Australia*

[3]*Deep Exploration Technologies Cooperative Research Centre, Mawson Building, University of Adelaide, SA 5005, Australia*

[4]*JRS Petroleum Research, Level 6, 28 Gawler Place, Adelaide, SA 5000, Australia*

**Corresponding author (e-mail: rosalind.king@adelaide.edu.au)*

Abstract: Delta–deepwater fold–thrust belts are linked systems of extension and compression. Margin-parallel maximum horizontal stresses (extension) on the delta top are generated by gravitational collapse of accumulating sediment, and drive downdip margin-normal maximum horizontal stresses (compression) in the deepwater fold–thrust belt (or delta toe). This maximum horizontal stress rotation has been observed in a number of delta systems. Maximum horizontal stress orientations, determined from 32 petroleum wells in the Gulf of Mexico, are broadly margin-parallel on the delta top with a mean orientation of 060 and a standard deviation of 49°. However, several orientations show up to 60° deflection from the regional margin-parallel orientation. Three-dimensional (3D) seismic data from the Gulf of Mexico delta top demonstrate the presence of salt diapirs piercing the overlying deltaic sediments. These salt diapirs are adjacent to wells (within 500 m) that demonstrate deflected stress orientations. The maximum horizontal stresses are deflected to become parallel to the interface between the salt and sediment. Two cases are presented that account for the alignment of maximum horizontal stresses parallel to this interface: (1) the contrast between geomechanical properties of the deltaic sediments and adjacent salt diapirs; and (2) gravitational collapse of deltaic sediments down the flanks of salt diapirs.

In many regions worldwide σ_H orientations are parallel or subparallel to absolute plate velocity vectors and ridge torques, for example, North America, South America and Western Europe (Richardson 1992; Zoback 1992). First-order intraplate stress patterns (wavelengths >1000 km) are therefore a result of large-scale plate boundary forces (e.g. ridge push, slab pull). The stress field generated by plate boundary forces are superimposed on major intra-plate sources of stress (gravitational forces imparted by mountain belts; lithospheric flexure) to generate the second-order stress pattern (wavelengths 100–500 km; Zoback 1992). However, recent years has seen significant advance in the understanding of short-wavelength (<100 km) third-order stress fields observed at the reservoir-, field- and basin-scale in sedimentary basins generated by local effects (e.g. topography, sediment loading, glacial rebound, elastic dislocation from large faults, overpressure generation, buckling, asperities on fault planes and lateral density contrasts; Bell 1996; Tingay *et al.* 2006; Heidbach *et al.* 2007; MacDonald *et al.* 2012). It is the relative magnitudes of the sources of stress that define the dominant stress regime in a given region (Zoback 1992; Bell 1996; Tingay *et al.* 2006). For example, a local stress source may induce large differential stresses that override the regional (far-field) stress source so that third-order stress patterns dominate in the area (e.g. Sonder 1990; Bell 1996; King *et al.* 2010*a*). Alternatively, a local stress source with low differential stresses may still affect stress orientations in regions where a layer with low shear strength (e.g. a detachment at the base of a delta system or a salt horizon) prevents the transfer of regional far-field stresses into layers where measurements are taken (Tingay *et al.* 2011; Bell 1996; King *et al.* 2010*b*).

Delta–deepwater fold–thrust belts (DDWFTBs) are linked systems of extension and compression (Morley 2003; Rowan *et al.* 2004; King *et al.* 2009; Fig. 1). Gravitational potential of accumulating sediment on the delta top generates margin-parallel maximum horizontal stress (σ_H) orientations (extension), which are marked by margin-parallel-striking normal growth faults and have listric shapes (Mandl

From: Healy, D., Butler, R. W. H., Shipton, Z. K. & Sibson, R. H. (eds) 2012. *Faulting, Fracturing and Igneous Intrusion in the Earth's Crust*. Geological Society, London, Special Publications, **367**, 141–153. http://dx.doi.org/10.1144/SP367.10

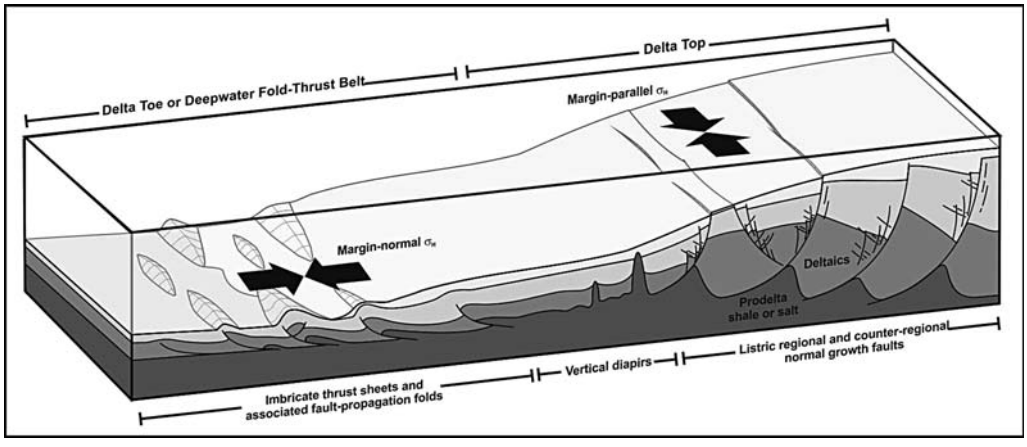

Fig. 1. Schematic diagram of a delta–deepwater fold–thrust belt illustrating the linked extension and compression. The delta top exhibits normal listric growth faults marking a margin-parallel maximum horizontal stress, and the delta toe (or deepwater fold–thrust belts) exhibits imbricate thrust sheets and associated fault-propagation folds marking a margin-normal maximum horizontal stress orientation (from King & Backé 2010).

& Crans 1981; Yassir & Zerwer 1997; King *et al.* 2009; Fig. 1). These extensional stresses drive downdip margin-normal σ_H orientations in the deepwater fold–thrust belt (or delta toe; compression), which are marked by margin-parallel-striking stacked thrust sheets and associated folds (Tingay *et al.* 2005; King *et al.* 2009; Fig. 1). However, the lobe shape of delta systems results in strike-slip stress regimes and associated structures at the outermost lateral margins of the systems (Peel *et al.* 1995). Present-day maximum horizontal stress orientations in the onshore Gulf Coast region display a clear margin-parallel trend (Tingay *et al.* 2006). However, margin-parallel σ_H orientations in the delta top region of the Gulf of Mexico, offshore Louisiana, demonstrate significant deflections from the expected margin-parallel σ_H orientations (Yassir & Zerwer 1997).

Maximum horizontal stress orientations in the Gulf of Mexico, offshore Louisiana, are third-order σ_H orientations generated by the gravitational potential of the accumulating sediment in the delta systems. However, many of these third-order σ_H orientations are deflected around salt diapirs that are considered to be caused by the contrast between the geomechanical properties of the salt and adjacent clastic deltaic sediments (Bell 1996; Yassir & Zerwer 1997). However, the Gulf of Mexico stress analysis conducted by Yassir and Zerwer (1997) was primarily a two-dimensional study using only the map pattern of σ_H orientations and does not account for the vertical changes in geomechanical properties or diapir shape. In this paper, we present 5 new σ_H orientations determined from 8 petroleum wells. We present a 3D model of the deflected σ_H orientations around a salt diapir, demonstrating changes in the orientations both laterally and vertically, and discuss the causes of these deflections.

Geological setting: the Gulf of Mexico

The Gulf of Mexico is one of the world's foremost petroleum provinces, and is located offshore the southern USA at 19–30°N and −83 to −97°W (Fig. 2a). Water depths in the Gulf of Mexico range from several metres around the coasts to more than 2000 m in the deep central parts. Much of the petroleum exploration has been focused on the shallow-water petroleum-rich delta top (Trudgill *et al.* 1999). Exploration focus shifted in the last decade to the deep water, as major discoveries in the deepwater fold–thrust belts were made (Trudgill *et al.* 1999). However, exploration and major reserve development programs continue in both the delta top and deepwater fold–thrust belt regions at present day.

The Gulf of Mexico is composed of several Upper Jurassic–Pleistocene delta systems that prograded from the north and west sourced by the Rio Grande (Galloway 1989; Fiduk *et al.* 1999; Fig. 2a). The delta systems sit on and above the Middle Jurassic Louann Salt, which is extensive across the northern Gulf of Mexico but is absent in the Mexican Ridges area (Peel *et al.* 1995; Trudgill *et al.* 1999). The Louann Salt forms the regional detachment zone beneath the deltaic sediments, with the majority of normal faults and thrust faults detaching at this level (Worrall & Snelson 1989;

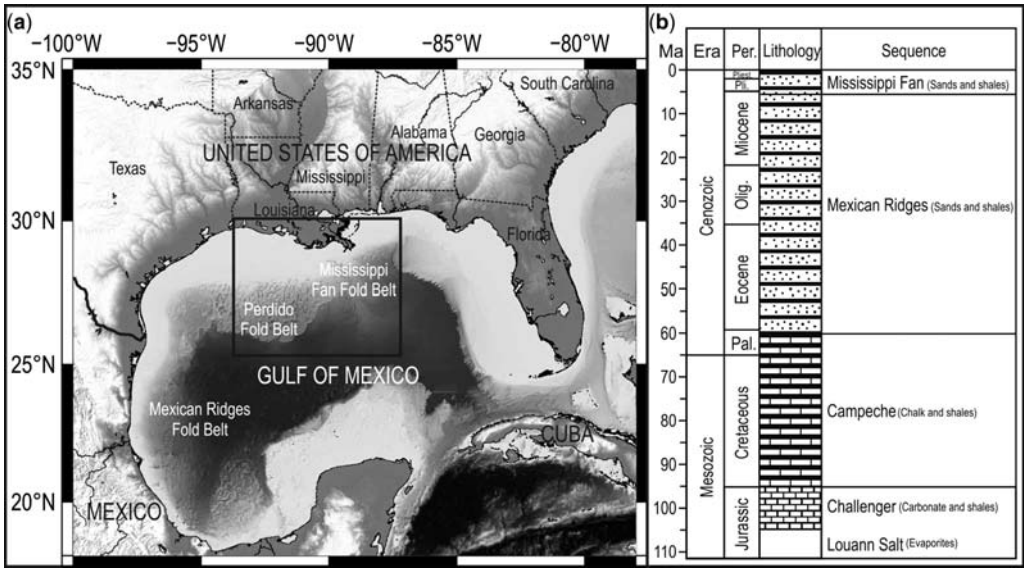

Fig. 2. (**a**) Location map of the Gulf of Mexico, offshore southern USA. Black box outlines the study area shown in Figure 4. (**b**) Mesozoic–Cenozoic tectonostratigraphy of the Gulf of Mexico (from Rowan 1997).

Wu *et al.* 1990; Rowan 1997; Fig. 1). Syn-rift sediments deposited on the rifted basement underlie the Louann Salt, but these are not well studied (Trudgill *et al.* 1999).

The post-salt stratigraphy can be divided into four broad sequences that demonstrate the evolution of the Gulf of Mexico from a shallow rifted margin in the Upper Jurassic–Early Cretaceous which continually subsided throughout the Late Cretaceous and into the Cenozoic to form the present-day shelf to basin-floor profile (Rowan 1997; Fiduk *et al.* 1999; Fig. 2). The carbonate Challenger and Campeche sequences demonstrate shallow marine environments across the Gulf of Mexico, but transition to deep marine in the present-day deepwater region during the Late Cretaceous (Weimer 1990; Feng & Buffler 1991; Rowan 1997; Fig. 2). The Palaeocene Mexican Ridges sequence is composed of deltaic sands on the present-day delta-top region and deepwater carbonates and turbidites in the present-day deepwater; the latter demonstrates bypass of deltaic sands to the basin floor (Weimer 1990; Feng & Buffler 1991; Rowan 1997; Fig. 2). The final sequence (the Palaeogene Mississippi Fan sequence) is a series of deltaic sands deposited on the present-day delta-top region and a deepwater turbidite sequence. This sequence is made up of several delta lobes (Weimer 1990; Feng & Buffler 1991; Rowan 1997; Fig. 2).

The accumulating sediment deformed by gravity sliding has resulted in a complex array of margin-parallel normal faults observed on the shelf, consistent with delta-top extension (Rowan 1997). Three fold–thrust belts generated by the updip extension are recognized in the deepwater: the Mississippi Fan Fold Belt, Perdido Fold Belt and the Mexican Ridges Fold Belt (Trudgill *et al.* 1999; Fig. 2a). It is therefore expected that σ_H orientations should rotate from margin-parallel on the delta top (marked by the margin-parallel normal faults) to margin-normal in the deepwater (marked by the imbricate thrust sheets) (e.g. King *et al.* 2009; Fig. 1).

Analysis of stress orientations in the Gulf of Mexico

Image logs and high-resolution dipmeter logs from 40 petroleum wells across the Gulf of Mexico were used to identify borehole failure and therefore determine the orientation of σ_H in 32 wells (this study; Yassir & Zerwer 1997). The orientation of σ_H can be determined from stress-induced compressive or tensile failure of the borehole wall, known as borehole breakout and drilling-induced tensile fractures (DITFs), respectively (Bell 1996; Fig. 3a).

Borehole failure

Borehole breakouts are a stress-induced elongation of the borehole cross-section. The presence of an open wellbore causes a localized perturbation of

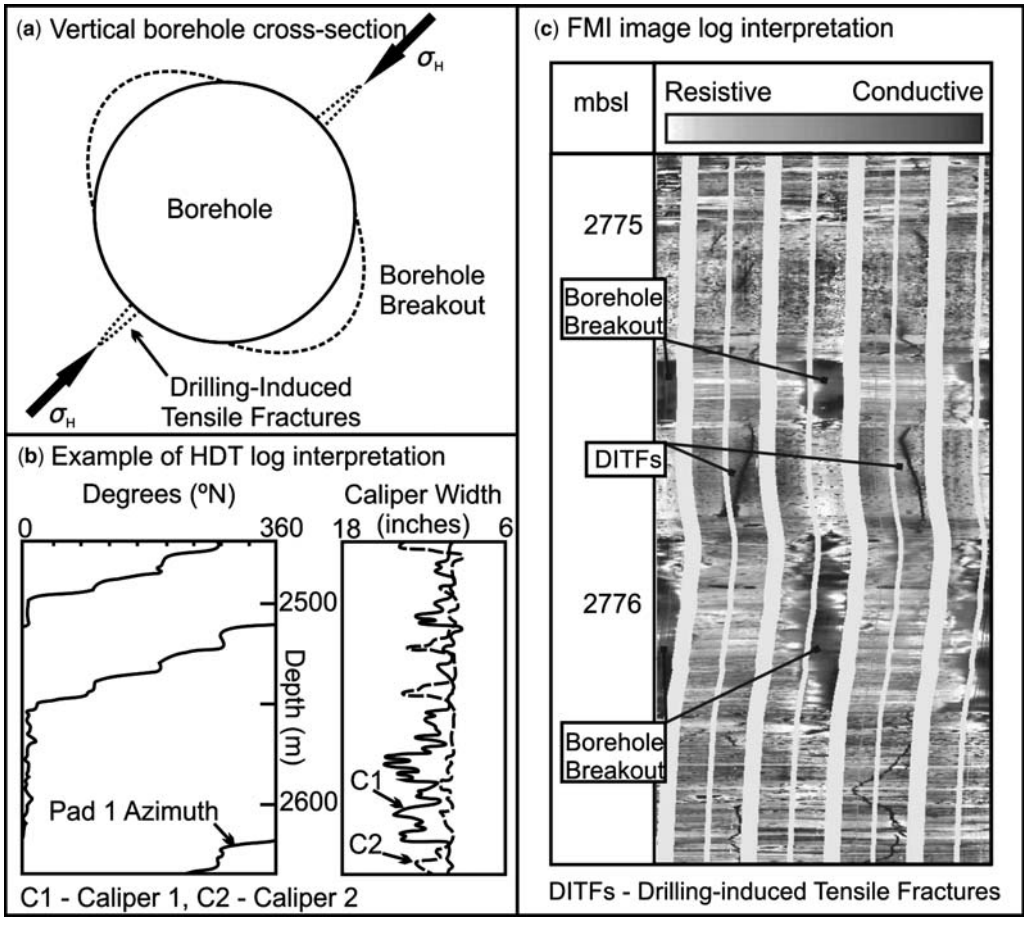

Fig. 3. (**a**) Borehole breakouts and drilling-induced tensile fractures observed on (**b**) dipmeter logs and (**c**) image logs can be used to determine the orientation of the maximum and minimum horizontal stresses (King *et al.* 2008). HDT, high-resolution dipmeter tool; FMI, formation micro-imaging tool; DITF, drilling-induced tensile fractures.

stresses in the vicinity of the borehole (Kirsch 1898). Borehole breakouts form when the maximum circumferential stress at the borehole wall exceeds the compressive rock strength, resulting in compressive failure and spalling of the borehole wall (Bell 1996). The circumferential stress is a function of the magnitude and anisotropy of σ_H and the minimum horizontal stress (σ_h) in vertical wells, with the maximum circumferential stress (and thus breakouts) developing perpendicular to the orientation of σ_H (e.g. Kirsch 1898; Bell & Gough 1979; Fig. 3a). Drilling-induced tensile fractures form due to tensile failure at the borehole wall when the minimum circumferential stress is less than the tensile strength of the borehole wall (Aadnoy & Bell 1998). Drilling-induced tensile fractures form parallel to the present-day σ_H orientation in vertical wells (Bell 1996; Brudy & Zoback 1999; Fig. 3a).

Borehole breakouts and DITFs may not directly yield the tectonic stress orientation in highly deviated boreholes due to the complex stresses that form around a borehole not oriented parallel to a principal stress (Mastin 1988; Peška & Zoback 1995). Hence, appropriate corrections to the orientations of borehole breakouts interpreted on the dipmeter or image logs were required in wells that were not vertical (after Peška & Zoback 1995).

Log interpretation

Resistivity image logs were used to interpret borehole breakout and DITF orientations in six petroleum wells. Borehole breakout orientations were

analysed from four-arm high-resolution dipmeter tools (composed of two pairs of calipers) in a further two petroleum wells in this study. Eight wells were combined with breakout orientations analysed from 27 wells by Yassir & Zerwer (1997). High-resolution dipmeter tools record borehole diameters in two orthogonal directions so borehole elongations, such as borehole breakouts, can be identified (Fig. 3b). The criteria used to successfully identify borehole breakouts on dipmeter logs are as follows (after Plumb & Hickman 1985).

- The rotation of the tool stops in the zone of elongation. The tool should rotate before and after the elongation. However, in zones of several small breakouts, the rotation may terminate completely.
- The difference recorded between the two arms of the calipers is >6 mm.
- The length (along the borehole axis) of the elongation is >1.5 m.
- The largest caliper should be extended greater than the drill bit size.
- The smallest caliper should not be significantly greater than the drill bit size.

Care is required when analysing dipmeter logs, so that borehole enlargements not related to stress (e.g. washouts or key seating) are not confused with borehole breakouts (e.g. Hillis & Williams 1993). Drilling-induced tensile fractures cannot be identified on dipmeter logs because they do not generally create borehole elongation.

Formation micro-image (FMI) and formation micro-scanning tools (FMS) produce an image of resistivity contrasts at the borehole wall (Ekstrom *et al.* 1987). The images show sedimentological, lithological and structural features such as cross-bedding and natural fractures. The images also exhibit drilling-related features such as tool marks, borehole breakout and DITFs. Borehole breakouts appear on resistivity image logs (in water-based muds) as pairs of conductive (dark) poorly resolved zones separated by 180°, and typically also exhibit caliper enlargement in the breakout direction (Fig. 3c). Drilling-induced tensile fractures appear on resistivity image logs as pairs of discontinuous, vertical, conductive (dark) fractures separated by 180° (Fig. 3c; Aadnoy & Bell 1998; Barton 2000).

Quality ranking stress orientations

The σ_H orientation for each well analysed in this study has been quality ranked in accordance with the standard World Stress Map quality ranking system (Table 1). The World Stress Map ranking system is based on the total number, the standard deviation and the total length of the stress indicators observed (Sperner *et al.* 2003; Heidbach *et al.* 2010; Table 1). The ranks are from A to E, with A being the highest quality and E the lowest (Table 1). Orientations that rank A–C are considered as reliable stress orientations for investigating primary stress fields under the World Stress Map ranking system (Zoback 1992). However, more recent studies in Cenozoic basins have argued that D-quality stress orientations can also provide important information, particularly when analysing third-order stress patterns or when multiple D-quality stress orientations are observed in close proximity (Tingay *et al.* 2010). Indeed, Yassir & Zerwer (1997) themselves presented an alternative ranking system for their work in the Gulf of Mexico, which locally ranked World Stress Map D-quality indicators as B and C quality. However, all stress orientations presented in Figure 4 are ranked according to the World Stress Map criteria (Sperner *et al.* 2003; Heidbach *et al.* 2010; Table 1).

New stress orientations in the Gulf of Mexico

Eight new petroleum wells have been analysed from the Gulf of Mexico in this study. All wells are located on the shelf within the delta-top region (Fig. 4). In total, 28 borehole breakouts and no DITFs were identified in the eight wells. The mean σ_H orientations from borehole breakouts were quality ranked with B- or C-quality stress orientations observed in two wells, D-quality orientations in three wells and the remaining three wells being ranked as E-quality (Table 2). The mean east–west σ_H orientation from these wells matches the expected margin-parallel σ_H orientation on the delta top of the idealized DDWFTB model (Fig. 1; Table 3). Indeed, σ_H orientations determined from wells 1, 2, 3 and 5 are all oriented subparallel to the Louisiana coastline, suggesting a typical delta-top margin-parallel σ_H orientation (Fig. 4).

The σ_H orientations determined from five petroleum wells of the eight examined here (Table 2) have been combined with σ_H orientations determined from 27 petroleum wells presented by Yassir & Zerwer (1997; Fig. 4). Table 3 presents the regional mean σ_H orientations determined for wells ranked A–C quality (considered reliable stress indicators; Zoback 1992) and for wells ranked A–D quality. Both studies suggest that present-day σ_H orientations on the delta top are oriented margin-parallel and are consistent with the stress field generated in the shelfal sections of a DDWFTB (Figs 1 & 4). All of the stress orientations presented in this study, including those from Yassir and Zerwer (1997), exhibited significantly high standard deviations in breakout orientations within each individual well. The high degree of scatter in borehole breakout orientations within individual wells is partially due to a combination of factors, such as

Table 1. *The World Stress Map quality ranking system for four- and six-arm high-resolution dipmeter logs (Sperner* et al. *2003) and resistivity and acoustic image logs (Heidbach* et al. *2010)*

	A quality	B quality	C quality	D quality	E quality
World Stress Map quality ranking system for four- and six-arm high resolution dipmeter logs					
No. borehole breakout	≥10	≥6	≥4	<4	0
Standard deviation (°)	≤12	≤20	≤25	>25	–
Combined length (m)	>300	>100	>30	<30	–
World Stress Map quality ranking system for resistivity or acoustic image logs					
No. borehole breakout/DITFs	≥10	≥6	≥4	<4	0
Standard deviation (°)	≤12	≤20	≤25	>25	–
Combined length (m)	>100	>40	>20	<20	–

the use of poorer quality four-arm caliper data in most wells. However, it is important to note that many wells exhibiting scattered breakout orientations are located on the shelf edge and slope where many salt diapirs are located (Yassir & Zerwer 1997).

Stress deflections in the Gulf of Mexico

Yassir & Zerwer (1997) identified several σ_H orientations that were not consistent with the expected margin-parallel orientation (Fig. 4). In this study, the σ_H orientation of 036 observed in well 4 is not consistent with this margin-parallel σ_H orientation (Fig. 4). Yassir & Zerwer (1997) identified that σ_H orientations were deflected away from the regional margin-parallel orientation near the interface between a salt diapir and the adjacent deltaic sediments (Fig. 4, areas 1 and 2). They hypothesized that the contrast in geomechanical properties between the salt and adjacent deltaic sediments resulted in σ_H orientations becoming locally rotated subparallel to the interface between the salt and the sediment (Bell 1996; Yassir & Zerwer 1997). The salt–sediment boundary is a surface that can sustain only a very weak shear force; principal stress azimuths are therefore deflected subparallel/subnormal to the salt–sediment interface (Davis & Engelder 1985). Yassir & Zerwer's (1997) interpretations were made using σ_H orientations determined from well

Table 2. *Maximum horizontal stress orientations determined in this study for 8 petroleum wells from the Gulf of Mexico, including the log type used for analysis, depth of tool run and the quality rank according to the World Stress Map quality ranking system (Table 1)*

Well	Water depth (m)	Tool	Vertical well deviation	Tool Runb (m bsl)	σ_H orientation	No. of stress indicator	Total length of indicators (m)	Standard deviation (°)	Quality
1 OCS-G 01666 018 ST01 BP00	145	FMI	60° to 030	1835–2143	100	9	46	18	B
2 OCS-G 1249 B-6ST2	34	HDT	<18°	758–2192	090	7	55	08	C
3 OCS-G 00244F-1	–	FMI	<8°	2582–3531	093	6	15	28	D
4 OCS-G 026#P-40 ST1	13	HDT	<25°	1800–2169	036	3	42	12	D
5 OSC-G 0310#201	6	FMI	<9°	1975–2840	102	3	11	15	D
6 OCS-G 01959 A015 ST01BP00	48	FMI	–	1067–3147	–	0	–	–	E
7 OCS-G 0390 040 ST00 BP01	14	FMI	–	4175–4328	–	0	–	–	E
8 OCS-G 0392 #Y29	–	FMI	–	1113–3764	–	0	–	–	E

Table 3. *Mean maximum horizontal stress orientations determined for A–C and A–D quality ranked wells from this study and Yassir & Zerwer (1997)*

Quality	No. of wells	σ_H orientation	Standard deviation (°)
Data from this study			
A–C	2	095	05
A–D	5	089	24
Data from Yassir & Zerwer (1997)			
A–C	11	039	49
A–D	27	043	51
Combined Data (this study and Yassir & Zerwer 1997)			
A–C	13	061	52
A–D	32	060	51

logs at depth combined with seafloor topography (e.g. areas 1 and 2 illustrated on Fig. 4) and therefore do not appreciate the 3D nature of the system. Here, we use time slices at 1 and 2 s from the Ship Shoal 3D seismic cube to demonstrate that the hypothesized rotations in the stress field adjacent to salt diapirs are also accurate when depth is considered.

Salt diapirs in the Ship Shoal 3D seismic cube are considered to be active or passive salt diapirs

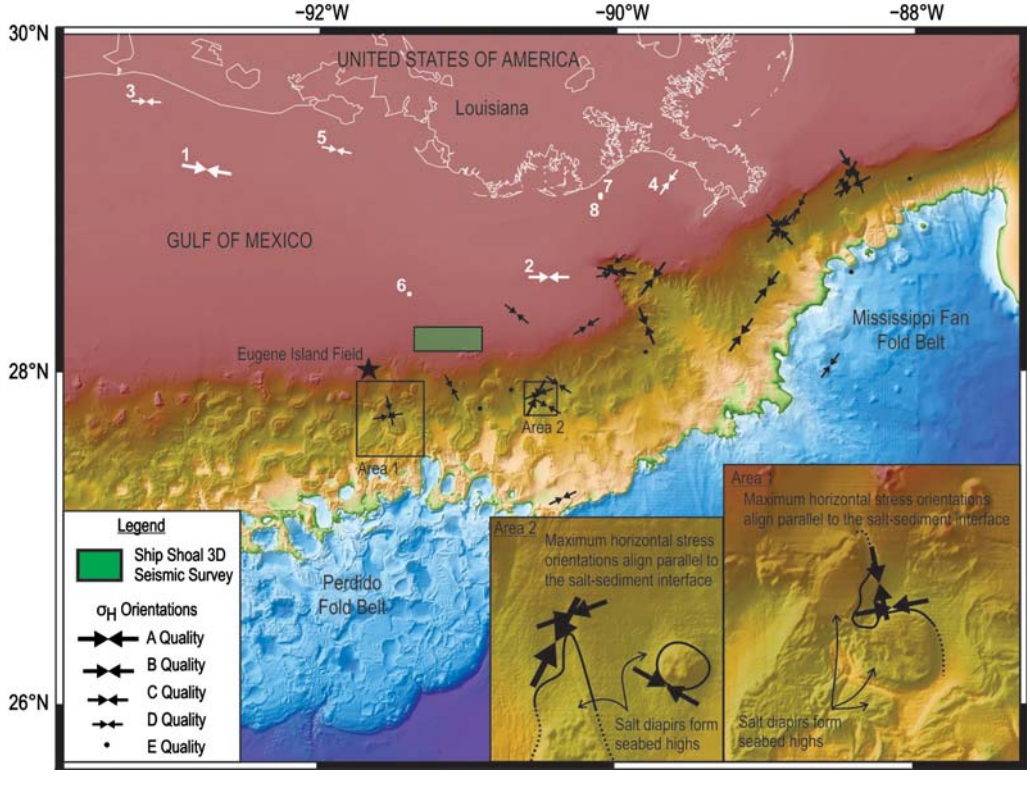

Fig. 4. Map illustrating the maximum horizontal stress orientations across the Gulf of Mexico (black arrows: Yassir & Zerwer 1997; white arrows: this study). The mean regional maximum horizontal stress orientation of 060 (standard deviation 51°) for all 27 A–D indicators is margin-parallel, consistent with the idealized model of a delta–deepwater fold–thrust belt (Fig. 1). Deflection of maximum horizontal stress orientations from margin-parallel occurs where salt diapirs pierce the deltaic sediments. The maximum horizontal stress orientations align parallel to the interface between salt and sediment, shown in areas 1 and 2.

(after Jackson *et al.* 1994). Active salt diapirs rise into overlying sediment by force, and are often associated with crestal collapse structures (Jackson *et al.* 1994). Passive diapirs rise by bouyancy into the overlying sediments and are accommodated without force; they therefore do not demonstrate any crestal collapse (Jackson *et al.* 1994). The salt diapirs have generated significant seafloor topography (Fig. 4). Time slices taken from at 1 and 2 s illustrate the shape of the salt diapirs at depth as conical structures with broad bases and narrow, domal crests (Fig. 5a, b). Figure 5 illustrates that salt diapir 1 becomes broader towards the east and west at depth and salt diapir 2 is elongated towards the north with increasing depth. Predictions of σ_H orientations at different depths around salt diapirs can be made using the time slices, following the hypothesis of Yassir & Zerwer (1997) that σ_H orientations are locally aligned subparallel to the interface between the salt diapirs and the adjacent deltaic sediments (Fig. 5a, b). At shallow depths, σ_H orientations are likely to deflect from the regional margin-parallel orientations over narrow areas which are associated with the narrow crests of salt diapirs (e.g. Fig. 5a). At greater depths, σ_H orientations are likely to deflect from the regional margin-parallel orientations over broader areas which are associated with the salt diapirs broad bases (e.g. Fig. 5b). Stress orientations in individual wells are consistent with depth and amount of lithification within deltaic sediments. This suggests that stress deflections are associated with large geomechanical contrasts in salt and clastic deltaic sediment, generating a surface that cannot sustain shear forces, and not subtle changes in the clastic deltaic sediments with depth. Furthermore, deflections of stress fields resulting in marked variations in fracture patterns around salt diapirs have also been imaged on time slices from Central Graben salt diapirs in the North Sea (e.g. Davison *et al.* 2000). Three-dimensional modelling was undertaken to better understand the geomechanical aspects controlling the observed local stress deflections near salt diapirs.

Numerical modelling of stress orientations around a salt diapir

The 3D modelling of the displacements, strain and stresses around the top of the Louann Salt, interpreted from the 3D Ship Shoal seismic cube (Fig. 6), was carried out using Poly3D, a 3D boundary element code using polygon elements and linear elasticity theory (Thomas 1993; Maerten *et al.* 2000,

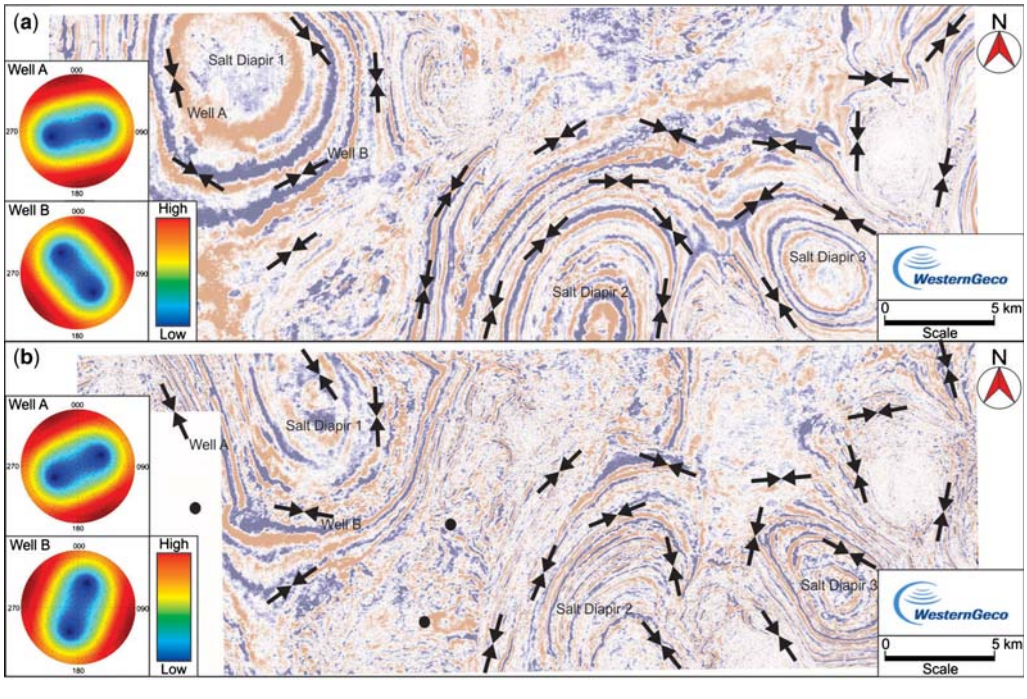

Fig. 5. Time slices taken from the Ship Shoal 3D seismic cube at (**a**) 1 s and (**b**) 2 s, demonstrating predicted maximum horizontal stress orientations (black arrows) and associated borehole stability diagrams for each orientation (vertical wells plot in the centre of the diagram, while horizontal wells plots on the circumference of the diagrams).

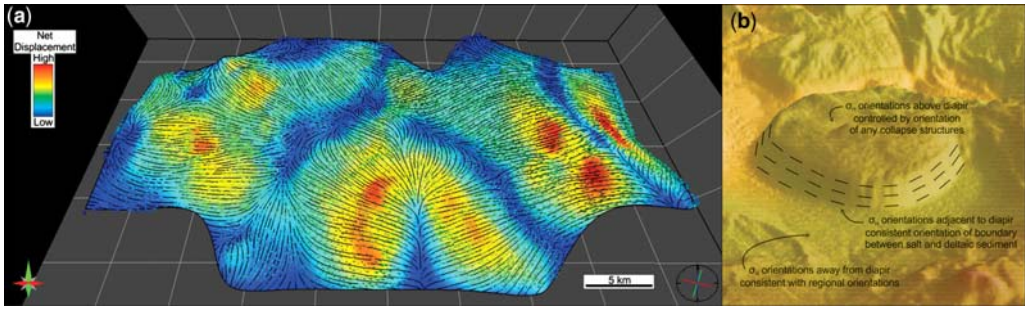

Fig. 6. (**a**) Poly3D model of the top Louann Salt horizon, interpreted from the Ship Shoal 3D seismic cube, demonstrating the displacement vectors (black lines) for the deltaic sediments at the interface between the salt diapirs and overlying sediments and the net displacement (with red being high and blue being low). Displacement vectors suggest movement will be downslope, with the greatest modelled displacement on the flanks of the salt diapirs. The predicted present-day displacement vectors are parallel to the present-day minimum horizontal stress and therefore perpendicular to the present-day maximum horizontal stress orientations (which lie in a horizontal plane) and parallel to the flanks of the salt diapirs. (**b**) A schematic 3D image of a conical salt diapir and the expected maximum horizontal stress deflections.

2002; Fiore *et al.* 2006; Maerten 2010). A boundary element method (BEM) greatly simplifies the model since only the discontinuities (such as faults or detachments) have to be taken into account and discretized. For the modelling purposes, the top Louann Salt was considered as a detachment system (i.e. a fault) and discretized with triangular elements with a 1000 m mesh size. Specific boundary conditions were applied, which govern how the elements should respond to far-field stress or strain states. The displacements were computed for a cohesionless detachment surface with boundary conditions set on the triangular boundary elements making up the faults as follows.

- The traction components parallel to the element plane in the dip direction and in the strike direction are both set to zero so the element surfaces may slip freely.
- The displacement discontinuity component normal to the element plane is set to zero to avoid opening or interpenetration of the fault surfaces.

This model examines the top Middle Jurassic Louann Salt, interpreted from the Ship Shoal 3D seismic cube (Fig. 6). The model was placed under a normal fault stress regime ($\sigma_v > \sigma_H > \sigma_h = 25$ MPa km$^{-1} > 20$ MPa km$^{-1} > 18$ MPa km^{-1}) consistent with an *in situ* stress magnitude study carried out in the Eugene Island field (Fig. 4; Finkbeiner *et al.* 2001). The resulting model suggests that the greatest net normal displacements occur on the flanks of salt diapirs, with displacement vectors for the deltaic sediments following the interface between the salt and deltaic sediments from the crest of the diapirs into the mini-basins between (black lines on Fig. 6). The model therefore implies deltaic sediments are sliding down the flanks of the salt diapirs. This gravitational collapse, under an extensional normal faulting stress regime, generates σ_H orientations that are perpendicular to the horizontal projection of the displacement vector; they will be aligned parallel to the strike of normal faults and to the flanks of salt diapirs. These observations are supported by outcrop analysis around exposed examples of diapiric flanks, which also reveals significant margin-parallel extensional faults (Alsop *et al.* 2000).

Implications for petroleum exploration and development

It has been demonstrated in previous studies that the orientations and magnitudes of present-day stresses are critical to borehole stability, water flooding, fracture stimulation and fault reactivation (e.g. Heffer & Lean 1993; Barton *et al.* 1998; Nelson *et al.* 2005; Tingay *et al.* 2009; King *et al.* 2010*c*). The evaluation of these implications can therefore become very difficult in settings such as the Gulf of Mexico, where the stress orientations are deflected away from the regional. Here we present examples of borehole stability from the Gulf of Mexico offshore Louisiana.

Boreholes can become unstable, in the form of borehole breakouts or DITFs, due to the anisotropy of the stress field. Boreholes are therefore most stable when drilled in a direction that subjects the well to the least stress anisotropy (Hillis & Williams 1993). In a normal fault stress regime on a delta top, as proposed to currently exist in the shelf region of the Gulf of Mexico, the greatest stress anisotropy occurs between the vertical stress ($\sigma_v = \sigma_1$) and

the minimum horizontal stress ($\sigma_h = \sigma_3$). Horizontal wells drilled towards the regional σ_H orientation (060 and 240) would therefore be typically considered to be least stable in a normal fault stress regime as they are subject to the greatest stress anisotropy (between σ_v and σ_h; Hillis & Williams 1993). The most stable wells will be vertical wells, as they are subject to the least stress anisotropy (between σ_H and σ_h) and have the lowest applied stress (Peška & Zoback 1995). Alternatively, if σ_H is close to σ_v then wells deviated towards σ_h will be most stable (e.g. Peška & Zoback 1995; Tingay *et al.* 2009). In the reverse (or thrust) fault stress regime of a deepwater fold–thrust belt, as proposed for the slope and basin-floor region of the Gulf of Mexico, the greatest stress anisotropy occurs between σ_H (σ_1) and σ_v (σ_3). Horizontal wells drilled towards the regional σ_h orientation (150 and 330) are therefore predicted to be least stable as they are subject to the greatest stress anisotropy (between σ_H and σ_v). The most stable wells are predicted to be horizontal wells drilled towards the σ_H direction (060 and 240), as they are subject to the least stress anisotropy (between σ_h and σ_v) and/or the lowest applied stress magnitude. However, if σ_h is high and close to σ_H, then vertical wells are more stable in a reverse fault stress regime (e.g. Peška & Zoback 1995).

On the shelf region of the Gulf of Mexico (delta top), vertical wells or wells deviated towards the σ_h direction are therefore least likely to be affected by borehole breakout or DITFs. On the slope and basin-floor region (deepwater fold–thrust belt), wells drilled parallel to the regional σ_H orientation (060 and 240) or vertical wells are least likely to be affected by borehole breakout or DITFs. These therefore represent the safest drilling directions, with respect to both borehole stability and fluid losses, on the delta top and in the deepwater fold–thrust belt, respectively. However, wells drilled adjacent to salt diapirs may not follow these predictions due to the local deflection of the stress field. In these cases, vertical wells are still likely to be the most stable; if horizontal wells are required, they must be drilled with respect to the deflection of the σ_H orientations expected near the interface between the salt diapirs and adjacent deltaic sediments (Fig. 5a, b).

Conclusions

We examined present-day stress orientations in eight new petroleum wells located in the delta top of the Gulf of Mexico offshore Louisiana. In total, 28 borehole breakouts were identified from image and high-resolution dipmeter tool (HDT) logs from five wells, giving a mean σ_H orientation of wells ranked A–D of 089 with a standard deviation of 24° (Fig. 4). The stress orientations interpreted here were combined with those from a further 28 wells analysed by Yassir & Zerwer (1997) to determine a regional mean σ_H orientation from 13 wells with A–C-quality stress orientations of 061, with a standard deviation of 52° (Fig. 4). The regional mean σ_H orientation, determined from A–D-quality mean stress orientations in 32 petroleum wells, is 060 with a standard deviation of 51° (this study; Yassir & Zerwer 1997; Fig. 4). These orientations are consistent with the delta-top margin-parallel σ_H orientations expected from the idealized model of a DDWFTB (Fig. 1).

Maximum horizontal stress orientations deflect from this regional margin-parallel orientation and align parallel around salt diapirs that have pierced through the overlying deltaic sediments (Fig. 4, areas 1 and 2). These deflections are attributed to the relative geomechanical contrasts that occur between 'weaker' salt diapirs and the adjacent 'stronger' deltaic sediments (e.g. Bell 1996; Yassir & Zerwer 1997). Using the Ship Shoal 3D seismic cube, we have demonstrated that deflections of σ_H orientations vary with depth due to the conical nature of the salt diapirs. A time slice taken at 1 s demonstrates that σ_H orientations deflect over narrow areas associated with narrow crests of salt diapirs, while large areas of deltaic sediment between the crests of the salt diapirs demonstrate the regional margin-parallel σ_H orientation (Figs 4 & 5a). In contrast, a time slice taken at 2 s demonstrates that σ_H orientations deflect over broad areas associated with wide bases of salt diapirs; only small areas of deltaic sediment between the bases of the salt diapirs demonstrate the regional margin-parallel σ_H orientation (Figs 4 & 5a).

A Poly3D model was constructed of the top Louann Salt from the Ship Shoal 3D seismic cube and a normal fault stress regime was applied, consistent with that determined in the Gulf of Mexico delta top (i.e. Finkbeiner *et al.* 2001). The model predicts that σ_H orientations are aligned parallel to the interface between salt diapirs and adjacent deltaic sediments, which is consistent with σ_H orientations determined from well data (Fig. 6). The model also predicts displacements vectors, which imply that the greatest net displacements on the interface between salt and sediment occur at the flanks of the salt diapirs (Fig. 6).

The orientations and magnitudes of present-day stresses are critical to borehole stability, water flooding, fracture stimulation and fault reactivation (e.g. Heffer & Lean 1993; Barton *et al.* 1998; Nelson *et al.* 2005; Tingay *et al.* 2009). In the Gulf of Mexico the most stable well on the delta top is vertical; unless σ_H is close to σ_v, then wells deviated towards σ_h are most stable. The most

stable well in the Gulf of Mexico delta toe (or deep-water fold–thrust belt) is deviated toward σ_H; unless σ_h is close to σ_H, then vertical wells are most stable. Knowledge of σ_H orientations in the Gulf of Mexico is critical for borehole stability studies due to the complex deflections of the regional margin-parallel σ_H orientations around salt diapirs. A single 'one case fits all' implied by the idealized model of a delta system (e.g. Fig. 1) does not apply for the Gulf of Mexico (Fig. 5). Careful consideration of the *in situ* stress field around salt diapirs is required.

The authors thank the reviewers for their helpful comments and the Australian Research Council for their financial support of this study. The authors would also like to thank Western Geoco for providing the Ship Shoal three-dimensional seismic cube and JRS Petroleum Research for the use of their software (JRS Suite).

References

Aadnoy, B. S. & Bell, J. S. 1998. Classification of drilling induced fractures and their relationship to in situ stress directions. *The Log Analyst*, **39**, 27–42.

Alsop, G. I., Brown, J. P., Davison, I. & Gibling, M. R. 2000. The geometry of drag zones adjacent to salt diapirs. *Journal of the Geological Society, London*, **157**, 1019–1029.

Barton, C. A. 2000. *Discrimination of natural fractures from drilling-induced wellbore failures in wellbore image data – implications for reservoir permeability*. Society of Petroleum Engineers International Petroleum Conference and Exhibition, Mexico.

Barton, C. A., Castillo, D. A., Moos, D., Peska, P. & Zoback, M. D. 1998. Characterising the full stress tensor based on observations of drilling-induced wellbore failures in vertical and inclined boreholes leading to improved wellbore stability and permeability prediction. *Australian Petroleum Production and Exploration Association Journal*, **38**, 467–487.

Bell, J. S. 1996. In situ stresses in sedimentary rocks (part 2): applications of stress measurements. *Geoscience Canada*, **23**, 135–153.

Bell, J. S. & Gough, D. I. 1979. Northeast-southwest compressive stress in Alberta: evidence from oil wells. *Earth and Planetary Science Letters*, **45**, 475–482.

Brudy, M. & Zoback, M. D. 1999. Drilling-induced tensile wall-fractures: implications for determination of in-situ stress orientation and magnitude. *International Journal of Rock Mechanics and Mining Sciences*, **36**, 191–215.

Davis, D. M. & Engelder, T. 1985. The role of salt in fold-and-thrust belts. *Tectonophysics*, **199**, 67–88.

Davison, I., Alsop, G. I. *et al.* 2000. Geometry and late-stage structural evolution of Central Graben salt diapirs, North Sea. *Marine and Petroleum Geology*, **17**, 499–522.

Ekstrom, M. P., Dahan, C. A., Chen, M. Y., Lloyd, P. M. & Rossi, D. J. 1987. Formation imaging with microelectrical scanning arrays. *The Log Analyst*, **28**, 294–306.

Feng, J. & Buffler, R. T. 1991. Preliminary age determinations for new deep Gulf of Mexico Basin sequences. *Gulf Coast Association of Geological Society Proceedings*, **41**, 283–289.

Fiduk, J. C., Weimer, P. *et al.* 1999. The Perdido Fold Belt, northwestern deep Gulf of Mexico, part 2: seismic stratigraphy and petroleum systems. *American Association of Petroleum Geologists Bulletin*, **83**, 578–612.

Fiore, P. E., Pollard, D. D., Currin, W. R. & Miner, D. M. 2006. Mechanical and stratigraphic constraints on the evolution of faulting at Elk hills, California. *American Association of Petroleum Geologists Bulletin*, **91**, 321–341.

Finkbeiner, T., Zoback, M., Flemings, P. & Stump, B. 2001. Stress, pore pressure, and dynamically constrained hydrocarbon columns in the South Eugene Island 330 field, northern Gulf of Mexico. *American Association of Petroleum Geologists Bulletin*, **85**, 1007–1031.

Galloway, W. E. 1989. Genetic stratigraphic sequences in basin analysis II: application to northwest Gulf of Mexico Cenozoic basin. *American Association of Petroleum Geologists Bulletin*, **73**, 143–154.

Heffer, K. J. & Lean, J. C. 1993. Earth Stress Orientation – A control on, and guide to, flooding directionality in a majority of reservoirs. *In*: Linville, W. (ed.) *Reservoir Characterisation III*, Pennwell Becks, Tulsa, 799–822.

Heidbach, O., Reinecker, J., Tingay, M., Müller, B., Sperner, B., Fuchs, K. & Wenzel, F. 2007. Plate boundary forces are not enough: second- and thrid-order stress patterns highlighted in the World Stress Map database. *Tectonics*, **26**, TC6014, doi: 10.1029/2007TC002133.

Heidbach, O., Tingay, M. R. P., Barth, A., Reinecker, J., Kurfeβ, D. & Müller, B. 2010. Global crustal stress pattern based on the 2008 World Stress Map database release. *Tectonophysics*, **482**, 3–15.

Hillis, R. R. & Williams, A. F. 1993. The stress field of the North West Shelf and wellbore stability. *Australian Petroleum Production and Exploration Association Journal*, **33**, 373–385.

Jackson, M. P. A., Vendeville, B. C. & Schulz-Ela, D. D. 1994. Salt-related structures in the Gulf of Mexico: a field guide for geophysicists. *The Leading Edge*, **13**, 837–842.

King, R. C. & Backé, G. 2010. A balanced 2D structural model of Hammerhead Delta—Deepwater Fold-Thrust Belt, Bight Basin, Australia. *Australian Journal of Earth Sciences*, **57**, 1005–1012.

King, R. C., Hillis, R. R. & Reynolds, S. D. 2008. In situ stresses and natural fractures in the Northern Perth Basin, Australia. *Australian Journal of Earth Sciences*, **55**, 685–701.

King, R. C., Hillis, R. R., Tingay, M. R. P. & Morley, C. K. 2009. Present-day stress and neotectonic provinces of the Baram Delta and deep-water fold-thrust belt. *Journal of the Geological Society, London*, **166**, 197–200.

King, R. C., Tingay, M. R. P., Hillis, R. R., Morley, C. K. & Clark, J. 2010*a*. Present-day stress orientations and tectonic provinces of the NW Borneo

collisional margin. *Journal of Geophysical Research*, **115**, B10415, doi: 10.1029/2009JB006997.

KING, R. C., BACKÉ, G., MORLEY, C. K., HILLIS, R. R. & TINGAY, M. R. P. 2010*b*. Balancing deformation in NW Borneo: quantifying plate-scale v. gravitational tectonics in a Delta and Deepwater Fold-Thrust Belt Systems. *Marine and Petroleum Geology*, **27**, 238–246.

KING, R. C., HILLIS, R. R., TINGAY, M. R. P. & DAMIT, A.-R. 2010*c*. Present-day stresses in Brunei, NW Borneo: superposition of deltaic and active margin tectonics. *Basin Research*, **22**, 236–247.

KIRSCH, V. 1898. Die Theorie der Elastizität und die Beddürfnisse der Festigkeitslehre. *Zeitschrift des Vereines Deutscher Ingenieure*, **29**, 797–807.

MAERTEN, F. 2010. Adaptive cross-approximation applied to the solution of system of equations and post-processing for 3D elastostatic problems using the boundary element method. *Engineering Analysis with Boundary Elements*, **34**, 483–491.

MAERTEN, L., POLLARD, D. D. & KARPUZ, R. 2000. How to constrain 3-D fault continuity and linkage using reflection seismic data: a geomechanical approach. *AAPG Bulletin*, **84**, 1311–1324.

MAERTEN, L., GILLEPIE, P. & POLLARD, D. D. 2002. Effects of local stress perturbation on secondary fault development. *Journal of Structural Geology*, **24**, 145–153.

MACDONALD, J., BACKÉ, G., KING, R., HOLFORD, S. & HILLIS, R. 2012. Geomechanical modelling of fault reactivation in ther Ceduna Sub-basin, Bight Basin, Australia. *In*: HEALY, D., BUTLER, R. W. H., SHIPTON, Z. K. & SIBSON, R. H. (eds) *Faulting, Fracturing and Igneous Intrusion in the Earth's Crust*. Geological Society, London, Special Publications, **367**, 71–89.

MANDL, G. & CRANS, W. 1981. Gravitational gliding in deltas. *In*: PRICE, N. J. & MCCLAY, K. R. (eds) *Nappe and Thrust Tectonics*. Geological Society, London, Special Publications, **9**, 41–54.

MASTIN, L. 1988. Effect of borehole deviation on breakout orientations. *Journal of Geophysical Research*, **93**, 9187–9195.

MORLEY, C. K. 2003. Mobile shale related deformation in large deltas developed on passive and active margins. *In*: VAN RENSBERGEN, P., HILLIS, R. R., MALTMAN, A. J. & MORLEY, C. K. (eds) *Subsurface Sediment Mobilization*. Geological Society, London, Special Publications, **216**, 335–357.

NELSON, E. J., HILLIS, R. R., MEYER, J. J., MILDREN, S. D., VAN NISPEN, D. & BRINER, A. 2005. The reservoir stress path and its implications for water flooding, Champion Southeast Field, Brunei. *Proceedings of Alaska Rocks the 40th US Symposium on Rock Mechanics*, American Rock Mechanics Association.

PEEL, F. J., TRAVIS, C. J. & HOSSACK, J. R. 1995. Genetic structural provinces and salt tectonics of the Cenozoic offshore U.S. Gulf of Mexico: a preliminary analysis. *In*: JACKSON, M. P. A., ROBERTS, D. G. & SNELSON, S. (eds) *Salt tectonics: A Global Perspective*. American Association of Petroleum Geologists, Tulsa, Memoir, **65**, 153–175.

PEŠKA, P. & ZOBACK, M. D. 1995. Compressive and tensile failure of inclined well bores and determination of in situ stress and rock strength. *Journal of Geophysical Research*, **100**, 12 791–12 811.

PLUMB, R. A. & HICKMAN, S. H. 1985. Stress induced borehole elongation: comparison between the four-arm dipmeter and the borehole televiewer in the Auburn geothermal well. *Journal of Geophysical Research*, **B90**, 5513–5521.

RICHARDSON, R. M. 1992. Ridge forces, absolute plate motions, and the intra-plate stress field. *Journal of Geophysical Research*, **97**, 11 739–11 748.

ROWAN, M. G. 1997. Three-dimensional geometry and evolution of a segmented detachment fold, Mississippi Fan foldbelt, Gulf of Mexico. *Journal of Structural Geology*, **19**, 463–480.

ROWAN, M. G., PEEL, F. J. & VENDEVILLE, B. C. 2004. Gravity-driven fold belts on passive margins. *In*: MCCLAY, K. R. (ed.) *Thrust Tectonics and Hydrocarbon Systems*. American Association of Petroleum Geologists, Tulsa, Memoir, **82**, 157–182.

SONDER, L. J. 1990. Effects of density contrasts on the orientation of stresses in the lithosphere: relation to principal stress directions in the Transverse ranges, California. *Tectonics*, **9**, 761–771.

SPERNER, B., MÜLLER, B., HEIDBACH, O., DELVAUX, D., REINECKER, J. & FUCHS, K. 2003. Tectonics stress in the Earth's crust: advances in the World Stress Map project. *In*: NIEUWLAND, D. A. (ed.) *New Insights into Structural Interpretation and Modelling*. Geological Society, London, Special Publications, **212**, 101–116.

THOMAS, A. L. 1993. *Poly3D: A three-dimensional, polygonal element, displacement discontinuity boundary element computer program with applications to fractures, faults, and cavities in the Earth's crust*. MS thesis, Stanford University.

TINGAY, M., MÜLLER, B., REINECKER, J., HEIDBACH, O., WENZEL, F. & FLECKENSTEIN, P. 2005. Understanding tectonic stress in the oil patch: the world stress map project. *The Leading Edge*, **24**, 1276–1282.

TINGAY, M., MÜLLER, B., REINECKER, J. & HEIDBACH, O. 2006. *State and orgin of the present-day stress field in sedimentary basins: New results from the World Stress Map Project*. 41st US Symposium on Rock Mechanics, Golden Rocks 2006, Published Plenary Paper ARMA/USRMS 06–1049.

TINGAY, M., HILLIS, R. R., MORLEY, C. K., KING, R. C., SWARBRICK, R. E. & DAMIT, A. R. 2009. Present-day stress and neotectonics of Brunei: implications for petroleum exploration and production. *American Association of Petroleum Geologists Bulletin*, **93**, 75–100.

TINGAY, M., MORLEY, C., KING, R., HILLIS, R., COBLENTZ, D. & HALL, R. 2010. Present-day stress field of southeast Asia. *In*: HEIDBACH, O., TINGAY, M. & WENZEL, F. (eds) *Frontiers of Stress Research*. Tectonophysics, Special Issue, **482**, 92–104.

TINGAY, M., BENTHAM, P., DE FEYTER, A. & KELLNER, A. 2011. Present-day stress field rotations associated with evaporites in the offshore Nile Delta. *GSA Bulletin*, **123**, 1171–1180.

TRUDGILL, B. D., ROWAN, M. G. *ET AL*. 1999. The Perdido Fold Belt, Northwestern Deep Gulf of Mexico, Part 1: Structural Geometry, Evolution and Regional Implications. *AAPG Bulletin*, **83**, 88–113.

WEIMER, P. 1990. Sequence stratigraphy, facies geometries, and depositional history of the Mississippi Fan, Gulf of Mexico. *AAPG Bulletin*, **74**, 425–453.

WORRALL, D. M. & SNELSON, S. 1989. Evolution of the northern Gulf of Mexico, with emphasis on Cenozoic growth faulting and the role of salt. *In*: BALLY, A. W. & PALMER, A. R. (eds) *The Geology of North America: an Overview*. Geological Society of America, Decade of North American Geology A, Geological Society of America, Boulder, CO, 97–138.

WU, S., BALLY, A. W. & CRAMEZ, C. 1990. Allochthonous salt, structure and stratigraphy of the north-eastern Gulf of Mexico, part II: structure. *Marine and Petroleum Geology*, **7**, 334–370.

YASSIR, N. A. & ZERWER, A. 1997. Stress regimes in the Gulf Coast, offshore Louisiana: data from well-bore breakout analysis. *American Association of Petroleum Geologists Bulletin*, **81**, 293–307.

ZOBACK, M. L. 1992. First- and second-order patterns of stress in the Lithosphere: the world stress map project. *Journal of Geophysical Research*, **97**, 11 703–11 728.